NATIONAL ADVISORY COMMITTEE
FOR AERONAUTICS

TECHNICAL NOTE

No. 1718

INFLUENCE OF LEADING-EDGE SUCTION ON LIFT-DRAG RATIOS

OF WINGS AT SUPERSONIC SPEEDS

By Clarence B. Cohen

Lewis Flight Propulsion Laboratory
Cleveland, Ohio

Washington
October 1948

NATIONAL ADVISORY COMMITTEE FOR AERONAUTICS

TECHNICAL NOTE No. 1718

INFLUENCE OF LEADING-EDGE SUCTION ON LIFT-DRAG RATIOS

OF WINGS AT SUPERSONIC SPEEDS

By Clarence B. Cohen

SUMMARY

A method based on linearized theory is presented for calculating the theoretical suction force at the subsonic leading edges of a family of wings at supersonic speeds. The method is used to determine the optimum sweepback angles for the tips of trapezoidal wings and to determine the effect of curvature of the tip contour on the lift-drag ratio of wing regions influenced by the tip. The effect of skin friction is included. The possible gain in lift-drag ratio from proper tip design of trapezoidal wings increases as the sweepback of the wing is increased. Results indicate that appropriately curved tip boundaries will give higher lift-drag ratios in the region affected by the tip than the best trapezoidal wing.

INTRODUCTION

The two-dimensional theory of thin airfoils at subsonic speeds gives a resultant force normal to the wing surface if only pressure forces on the wing surface are considered, which implies a net drag. For this theory, however, the velocity components become infinite at the leading edge. Evaluation of the effect of this singularity yields a suction force that exactly cancels the drag and thus satisfies the momentum requirement that the resultant force vector be normal to the direction of flight (reference 1).

The procedure used to derive the suction force is not restricted to two-dimensional wings and indicates that such a force may occur along any edge at which the normal component of the velocity becomes infinite. In the linearized theory for thin wings flying at supersonic speeds, such a singularity exists along leading edges swept behind the Mach angle. It has therefore been proposed by Brown (reference 2) that a leading-edge suction force, which tends to counteract the wave drag, exists along subsonic leading edges of wings flying at supersonic speeds. The magnitude of this force is calculated in reference 2 for triangular wings

swept beyond the Mach angle. The reduction in drag predicted by
the concept of leading-edge suction force has been shown by
Vincenti to occur experimentally for triangular wings swept beyond
the Mach angle.

The perturbation-velocity components required to evaluate the
local leading-edge suction force may be obtained by the methods of
reference 3 for the class of wings or wing tips for which the for-
ward Mach line from the subsonic leading edge intersects a super-
sonic leading edge. An analysis of the suction force for such
wings was made at the NACA Cleveland laboratory in 1948 to deter-
mine its effect on the lift-drag ratio obtainable with various tip
contours.

SYMBOLS

The following symbols are used in this report:

b constant defining location of trailing edge of wing

$C_{D,f}$ coefficient of drag due to skin friction

C_L lift coefficient

C_p pressure coefficient

c chord of wing

D drag force

F suction force (in flight direction)

G quantity defining φ_n

k constant defining angle of straight wing edge

L lift force

M Mach number (free stream)

n distance normal to leading edge

q dynamic pressure, $\frac{1}{2}\rho U^2$

R   distance ratio, $\dfrac{v - v_1(u_2)}{u - u_2} = \dfrac{V}{u - u_2}$

S   integration area

s   distance along wing edge

U   free-stream velocity

u, v   oblique coordinates

V   distance (in v-direction) between subsonic and supersonic leading edges

x, y   Cartesian coordinates

α angle of attack, radians

β cotangent of Mach angle, $\sqrt{M^2 - 1}$

ϵ semiapex angle of triangular wing

θ angle between wing edge and flight direction (positive counterclockwise), $\dfrac{dy}{dx}$

μ Mach angle, $\sin^{-1}\dfrac{1}{M}$

ρ mass density of air

φ perturbation-velocity potential

Subscripts:

1   supersonic leading edge

2   subsonic leading edge

f   friction

n   indicates direction normal to wing leading edge

t   tip point of wing (at greatest span)

w   wave

x, y   indicates velocity components in x, y directions

DERIVATION OF EXPRESSION FOR LEADING-EDGE SUCTION FORCE

In subsonic airfoil theory, the form of the equation of the velocity component normal to the leading edge (reference 1) is

$$\varphi_n = \frac{G}{\sqrt{n}} \qquad (1)$$
$$\scriptstyle n \to 0$$

where $\varphi_n = \frac{\partial \varphi}{\partial n}$ is the perturbation velocity in the n direction (fig. 1). Thus φ_n approaches infinity as n approaches zero. Analysis of this singularity results in a suction force per unit length, which can be expressed in differential form as (reference 1)

$$\frac{dF_n}{ds} = \pi \rho G^2 \qquad (2)$$

where s is distance along the wing edge (fig. 1).

Equations (1) and (2) may be rewritten, as in reference 2, to include the effects of compressibility.

$$\varphi_n = \frac{G}{\sqrt{n}} \frac{1}{\sqrt{1-M_n^2}} \qquad (1a)$$
$$\scriptstyle n \to 0$$

and

$$\frac{dF_n}{ds} = \frac{\pi \rho G^2}{\sqrt{1-M_n^2}} \qquad (2a)$$

where M_n is the component of the Mach number normal to the edge.

For subsonic two-dimensional wings, the factor G is such that the force defined by equation (2a) is just sufficient to cancel the drag resulting from the flat-plate analysis. For supersonic wings, the factor G must be determined from the appropriate value of φ_n at the subsonic leading edge. From reference 3, the perturbation-velocity components in the x and y directions near the leading edge can be written (appendix A) as

$$\left.\begin{array}{l} \varphi_x = \dfrac{U\alpha}{\beta\pi} \left(1 - \dfrac{du_2}{dv}\right) \sqrt{\dfrac{v-v_1(u_2)}{u-u_2}} \\[2em] \underset{n\to 0}{} \\[1em] \varphi_y = -\dfrac{U\alpha}{\pi} \left(1 + \dfrac{du_2}{dv}\right) \sqrt{\dfrac{v-v_1(u_2)}{u-u_2}} \\ \underset{n\to 0}{} \end{array}\right\} \qquad (3)$$

The coordinate system used herein is shown in figure 1. The relations between the oblique and Cartesian coordinates are given by

$$\left.\begin{array}{ll} u = \dfrac{M}{2\beta}\,(x-\beta y) & v = \dfrac{M}{2\beta}\,(x+\beta y) \\[2em] x = \dfrac{\beta}{M}\,(v+u) & y = \dfrac{1}{M}\,(v-u) \end{array}\right\} \qquad (4)$$

Equations (3) may be combined to obtain the normal velocity component near the edge

$$\varphi_n = \dfrac{U\alpha}{\beta\pi} \sqrt{R\left[\left(1 - \dfrac{du_2}{dv}\right)^2 + \beta^2\left(1 + \dfrac{du_2}{dv}\right)^2\right]} \qquad (5)$$
$$\underset{n\to 0}{}$$

where

$$R = \dfrac{v-v_1(u_2)}{u-u_2} = \dfrac{V}{u-u_2}$$

The geometrical relation between R and n as $n\to 0$ is shown in figure 2, where

$$n = \overline{PQ}\,\sin(\theta+\mu) = \dfrac{V}{R}\,\sin(\theta+\mu) \qquad (6)$$

The following expressions are derived from the relations between the oblique and Cartesian coordinates:

$$\sin\theta = \frac{\left(1 - \dfrac{du_2}{dv}\right)}{\sqrt{\left(1 - \dfrac{du_2}{dv}\right)^2 + \beta^2\left(1 + \dfrac{du_2}{dv}\right)^2}}$$

$$\cos\theta = \frac{\beta\left(1 + \dfrac{du_2}{dv}\right)}{\sqrt{\left(1 - \dfrac{du_2}{dv}\right)^2 + \beta^2\left(1 + \dfrac{du_2}{dv}\right)^2}} \quad\quad (7)$$

$$ds = \sqrt{(dx)^2 + (dy)^2} = \frac{dv}{M}\sqrt{\left(1 - \dfrac{du_2}{dv}\right)^2 + \beta^2\left(1 + \dfrac{du_2}{dv}\right)^2}$$

With the aid of equations (6) and (7), equations (1a) and (5) may be solved for G^2.

$$G^2 = \left(\frac{8U^2\alpha^2V\beta}{\pi^2 M}\right)\frac{\dfrac{du_2}{dv}}{\sqrt{\left(1 - \dfrac{du_2}{dv}\right)^2 + \beta^2\left(1 + \dfrac{du_2}{dv}\right)^2}} \quad\quad (8)$$

This value of G^2 substituted into equation (2a) yields the normal force per unit length along the wing edge.

$$\frac{dF_n}{ds} = \frac{4\rho U^2\alpha^2 V}{\pi M}\sqrt{\frac{du_2}{dv}} \quad\quad (9)$$

With the use of the relation

$$\frac{dF}{dv} = \frac{dF}{ds}\frac{ds}{dv} = \frac{dF_n}{ds}\frac{ds}{dv}\sin\theta$$

there results

$$\frac{dF}{dv} = \frac{4\rho U^2 \alpha^2 v}{\pi M^2} \left(1 - \frac{du_2}{dv}\right) \sqrt{\frac{du_2}{dv}} \tag{10}$$

The leading-edge suction force can now be expressed in integral form as

$$F = \frac{4\rho U^2 \alpha^2}{\pi M^2} \int v \left(1 - \frac{du_2}{dv}\right) \sqrt{\frac{du_2}{dv}} \, dv \tag{11}$$

The quantity $\left(1 - \frac{du_2}{dv}\right) \sqrt{\frac{du_2}{dv}}$ in equation (11) is given in figure 3 as a function of θ for three values of β. With the aid of curves such as these and a drawing of the wing in question, equation (11) may be evaluated by a numerical summation.

The force defined by equation (11) is obtained when the radius of curvature of the leading edge is vanishingly small and when the velocity components normal to the edge become infinite at the edge. In practice, however, the infinite velocity components predicted by linearized theory correspond to a high negative pressure coefficient near the edge. By rounding the subsonic leading edge to increase the projected area on which the lower pressure can act, it is possible to reduce the total drag of the wing. As the edge radius is increased, an optimum curvature that corresponds to a maximization of the product of area times suction force per unit area, should be obtained. It has been shown experimentally that rounding the leading edge of triangular wings swept beyond the Mach angle increases the lift-drag ratio, but that continued rounding beyond a certain value produces no further gains.

APPLICATION OF LEADING-EDGE SUCTION-FORCE EQUATION

For a given main surface (fig. 1), the optimum wing is one whose tip has the greatest lift-drag ratio L/D. If the tip has no subsonic edge, this ratio is simply $\dfrac{L}{D} = \dfrac{L}{D_w + D_f} = \dfrac{\dfrac{1}{\alpha}}{1 + \dfrac{D_f}{D_w}}$ where

D_w is the wave drag and D_f the skin-friction drag. If the tip has a subsonic leading edge its lift-drag ratio becomes

$$\frac{L}{D} = \frac{L}{D_w + D_f - F} = \frac{1}{\alpha}\left(\frac{1}{1 + \dfrac{D_f}{D_w} - \dfrac{F}{D_w}}\right) \tag{12}$$

where F is the suction force at the subsonic leading edge. The tip with the minimum value of $\left(\dfrac{D_f}{D_w} - \dfrac{F}{D_w}\right)$ therefore has the highest lift-drag ratio. If frictionless flow is assumed, the parameter F/D_w should be maximized.

As an example of the procedure for obtaining wings of optimum plan boundaries, the quantity $\left(\dfrac{D_f}{D_w} - \dfrac{F}{D_w}\right)$ will be derived for a wing with a straight-line supersonic leading edge $v_1 = k_1 u$. The quantity V in equation (11) then becomes $v - k_1 u_2$ (fig. 4) and the suction force is

$$F = \frac{4\rho U^2 \alpha^2}{\pi M^2} \int_0^{v_t} (v - k_1 u_2)\left(1 - \frac{du_2}{dv}\right)\sqrt{\frac{du_2}{dv}}\, dv \tag{13}$$

where v_t is the value of v at the extreme tip and $u = u_2(v)$ is the equation of the tip edge.

The wave drag for a wing tip of this type is (appendix B)

$$D_w = \frac{4\rho U^2 \alpha^2}{\pi M^2 k_1 \sqrt{-k_1}} \int_0^{v_t} \left\{\left[1 + k_1\left(1 - 2\frac{du_2}{dv}\right)\right]\sqrt{(v - k_1 u_2)\left[b - (v - k_1 u_2)\right]}\right.$$

$$\left. + (k_1 - 1)b \tan^{-1}\sqrt{\frac{b - (v - k_1 u_2)}{(v - k_1 u_2)}}\right\} dv \tag{14}$$

and the friction drag is

$$D_f = C_{D,f} \frac{1}{2} \rho U^2 \times (\text{tip area}) = \frac{\beta C_{D,f} \rho U^2}{-k_1 M^2} \int_0^{v_t} \left[b - (v - k_1 u_2) \right] dv \tag{15}$$

The constant b in the equation for the trailing edge determines the chord of the wing (fig. 4). Then combining equations (13) to (15)

$$\left(\frac{D_f}{D_w} - \frac{F}{D_w} \right) = \frac{-\frac{\pi}{4} \frac{\beta C_{D,f}}{\alpha} \sqrt{-k_1} \int_0^{v_t} \left[b - (v - k_1 u_2) \right] dv - k_1 \sqrt{-k_1} \int_0^{v_t} \left[(v - k_1 u_2)\left(1 - \frac{du_2}{dv} \right) \sqrt{\frac{du_2}{dv}} \right] dv}{\int_0^{v_t} \left\{ \left[1 + k_1\left(1 - 2\frac{du_2}{dv} \right) \right] \sqrt{(v - k_1 u_2)\left[b - (v - k_1 u_2) \right]} + (k_1 - 1)b \tan^{-1} \sqrt{\frac{b - (v - k_1 u_2)}{(v - k_1 u_2)}} \right\} dv} \tag{16}$$

If the wing-tip equation is kept in the general form $u_2(v)$, the conditions for minimizing equation (16) can only be indicated. The procedure is to set the differential of equation (16) equal to zero; the solution to the resulting integral equation, however, has not yet been determined.

If the wing is assumed to have a straight tip edge given by $u_2 = k_2 v$, then the plan form is a trapezoid and the integrals in equation (16) can be evaluated (appendix C) to yield

$$\frac{D_f - F}{D_w} = \frac{-\dfrac{\beta C_{D,f}}{\alpha^2} \sqrt{-k_1} - \dfrac{4}{\pi}(1-k_2)\, k_1 \sqrt{-k_1 k_2}}{\left(3k_1 - 2k_1 k_2 - 1\right)} \tag{17}$$

where

$$-\infty < k_1 < 0$$

$$0 < k_2 < 1$$

and k_1 and k_2 determine the sweep angles of the leading and trailing edges θ_1 and θ_2, respectively. The angles corresponding to several values of the constants are:

k_1	θ_1	k_2	θ_2
0	$-\mu$	0	μ
-1	$\pi/2$	1	0
$-\infty$	μ		

The equations relating the angles and the constants are

$$\left.\begin{aligned}
\theta_1 &= \tan^{-1}\frac{(k_1 - 1)}{\beta(k_1 + 1)} \\[2ex]
\theta_2 &= \tan^{-1}\frac{(1 - k_2)}{\beta(1 + k_2)}
\end{aligned}\right\} \tag{18}$$

As an indication of the variation of leading-edge suction force for this type of wing, the effect of θ_2 upon F/D_w, as calculated from equations (17) and (18) with $C_{D,f} = 0$, is shown in figure 5 for $\theta_1 = 65^\circ$ $(k_1 = -2.75)$ at $M = \sqrt{2}$. An optimum value of θ_2 occurs at about 20°.

In order to obtain an expression for optimum values of θ_2 (or k_2) as a function of k_1, equation (17) must be differentiated and set equal to zero. When differentiated with respect to k_2, the equality yields

$$2k_2{}^2 k_1 + k_2 (3-7k_1) + 3k_1 - 1 + \frac{\pi \beta C_{D,f}}{\alpha^2} \sqrt{k_2} = 0 \qquad (19)$$

Differentiation with respect to k_1 yields no true maximum for the type of wing treated. The variation of the optimum value of k_2 with k_1, as expressed by equation (19), is shown in figure 6 for several values of $\dfrac{\beta C_{D,f}}{\alpha^2}$.

A wing with $\theta_1 = 65^\circ$ and three alternate tip curves A, B, and C passing through points O and t is shown in figure 7. Tip curve B is swept so that $\theta_2 = 20^\circ$ (the optimum for this trapezoidal wing from fig. 5). Curves A and C are arbitrary curves, symmetrical about B, drawn through O and t.

The following values of F/D_w were obtained by numerical integration of equations (13) and (14) for these tips; the resulting effect on lift-drag parameter $\alpha L/D$ for frictionless flow is also shown:

Wing	F/D_w	$\alpha L/D$ (frictionless flow)
A	0.39	1.64
B	.31	1.45
C	.20	1.25

These results indicate that the lift-drag ratio may be increased by the use of appropriately curved wing boundaries at supersonic speeds.

As an indication of the magnitudes of F/D_w theoretically obtainable with other type plan forms, the variation of F/D_w with apex angle for a triangular wing is shown in figure 8. This relation is based on the equations in reference 2.

The variation of maximum lift-drag ratio with k_1 is shown in figure 9 for trapezoidal tips. These lift-drag ratios were calculated from the optimum values of k_2 shown in figure 6.

The lift-drag ratio for the main surface of a trapezoidal wing is
also shown for comparison. These curves show that the maximum
lift-drag ratio of sweptback trapezoidal wings is obtained, not
when the wing is cut off at the inner Mach line (main-surface
curves), but rather when the optimum tip angle, based on considera-
tion of leading-edge suction, is chosen. (This result held for all
values of the friction parameter $\dfrac{\beta C_{D,f}}{\alpha^2}$ shown.) For sweptforward
trapezoidal wings, however, figure 9 indicates that the optimum
lift-drag ratio L/D is obtained when the tip is cut back at the
inner Mach angle.

The lift-drag ratio is shown in figure 10 as a function of
angle of attack for the wing tips previously mentioned, for the
main surface, and for a tip cut off in the flow direction (tip D).
The calculations were made for $M = \sqrt{2}$ and $C_{D,f} = 0.005$. This
figure indicates that appropriately curved plan forms give more
favorable lift-drag ratios than the optimum trapezoidal wing. For
wings of low aspect ratio, the effect of the tip design becomes
relatively more important; a complete study must therefore include
the effect of aspect ratio. From the standpoint of high lift-drag
ratio, a tip such as D (fig. 10) is poor for any aspect ratio
inasmuch as a higher lift-drag ratio can be obtained merely by
cutting off the wing at the Mach line.

                              CONCLUSIONS

        The following conclusions result from a method for evaluation
of the theoretical leading-edge suction force on a type of wing
for which the forward Mach lines from the subsonic leading edge
intersect a supersonic leading edge:

        1. The optimum lift-drag ratio of sweptback trapezoidal wings
is obtained when the optimum tip angle, based on consideration of
leading-edge suction, is chosen. For sweptforward trapezoidal
wings, however, the optimum lift-drag ratio is obtained when the
tip is cut back at the Mach angle. The possible gain in lift-drag
ratio from proper tip design of trapezoidal wings increases as the
sweepback of the wing is increased.

        2. Higher lift-drag ratios may be obtained with wing tips
whose edges are appropriately curved than may be obtained with
straight-line wing tips.

Lewis Flight Propulsion Laboratory,
        National Advisory Committee for Aeronautics,
                Cleveland, Ohio, July 15, 1948.
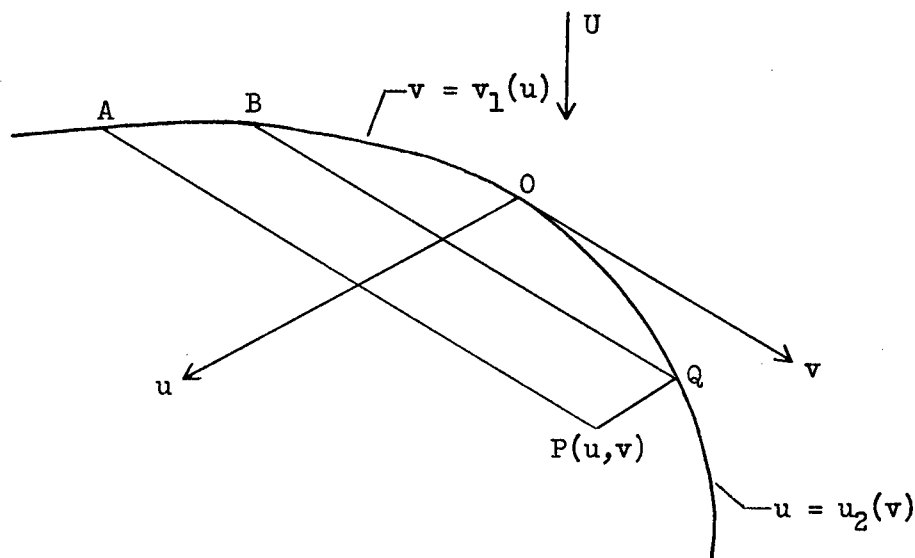
1001

APPENDIX A

PERTURBATION-VELOCITY COMPONENTS

NEAR SUBSONIC LEADING EDGE

The x-component of the perturbation velocity $\varphi_x = \dfrac{\partial \varphi}{\partial x}$, where φ is the perturbation-velocity potential, is given in reference 3 as

$$\frac{\partial \varphi}{\partial x} = \frac{U\alpha}{2\beta\pi} \int_{AB} \frac{dv'-du'}{\sqrt{(u-u')(v-v')}} - \frac{U}{2\beta\pi} \int_{BQ} \frac{(-\alpha)\left(1 - \dfrac{du_2}{dv}\right)dv'}{\sqrt{(u-u')(v-v')}} \quad (A1)$$

where the primes denote the variables of integration.

The integrals are evaluated along the supersonic leading edge from A to B and along the Mach line from B to Q. When point P approaches the subsonic leading edge $\widehat{OQ}$ $(n \to 0)$, points A and B converge and equation (A1) reduces to

$$\varphi_x = \frac{U\alpha}{2\beta\pi} \left(1 - \frac{du_2}{dv}\right) \int_{BQ} \frac{dv'}{\sqrt{(u-u')(v-v')}} \qquad (A2)$$

$$n \to 0$$

which upon integration becomes the first of equations (3). The expression for φ_y is obtained similarly.

APPENDIX B

DRAG FORCE

In accordance with linearized theory, the wave drag of a thin flat plate is

$$D_w = \alpha L = \alpha C_L q S \tag{B1}$$

where the lift coefficient can be expressed as

$$C_L = \frac{-2 \displaystyle\iint C_p \, dS}{\displaystyle\iint dS} \tag{B2}$$

For a wing of the type shown in figure 4, reference 3 shows that the pressure coefficient can be expressed as

$$C_p = -\frac{2\alpha}{\pi\beta}\left[\left(1 - \frac{du_2}{dv}\right)\sqrt{\frac{v - k_1 u_2}{u - u_2}} + \frac{1 - k_1}{\sqrt{-k_1}} \tan^{-1} \sqrt{\frac{k_1(u_2 - u)}{v - k_1 u_2}}\right] \tag{B3}$$

A combination of equations (B1) to (B3) yields

$$D_w = \frac{4\alpha^2 \rho U^2}{\pi M^2} \int_0^{v_t} dv \int_{u_2(v)}^{\frac{v-b}{k_1}} \left[\left(1 - \frac{du_2}{dv}\right)\sqrt{\frac{v - k_1 u_2}{u - u_2}} + \frac{1 - k_1}{\sqrt{-k_1}} \tan^{-1} \sqrt{\frac{k_1(u_2 - u)}{v - k_1 u_2}}\right] du \tag{B4}$$

which upon integration with respect to u becomes equation (14).

APPENDIX C

SUCTION FORCE AND DRAG FOR A TRAPEZOIDAL WING

The equation of the tip of a trapezoidal wing is

$$u_2(v) = k_2 v \tag{C1}$$

By the use of this equation, if the value of v_t is known, the wave drag, friction drag, and suction force can be obtained from equations (13) to (15). For the trapezoidal wing

$$v_t = \left(\frac{c}{1-k_1 k_2}\right) \frac{M \sqrt{M^2(k_1 + 1)^2 - 4k_1}}{2\beta} \tag{C2}$$

The use of equations (C1) and (C2) in equations (13) to (15) yields

$$F = \frac{\rho U^2 \alpha^2 c^2}{2\pi \beta^2} \frac{(k_2 - 1)\sqrt{k_2}}{(k_2 k_1 - 1)} \left[M^2(k_1 + 1)^2 - 4k_1\right] \tag{C3}$$

$$D_w = \frac{\rho U^2 \alpha^2 c^2}{8\beta^2} \left\{ \frac{\left[M^2(k_1 + 1)^2 - 4k_1\right](3k_1 - 2k_1 k_2 - 1)}{(1-k_1 k_2)\, k_1 \sqrt{-k_1}} \right\} \tag{C4}$$

$$D_f = \frac{\rho U^2 c^2 C_{D,f}}{8\beta} \frac{\left[M^2(k_1 + 1)^2 - 4k_1\right]}{k_1(k_1 k_2 - 1)} \tag{C5}$$

By subtracting equation (C3) from (C5) and by dividing the result by equation (C4), equation (17) is obtained.

REFERENCES

1. von Kármán, Th. and Burgers, J. M.: General Aerodynamic Theory -
   Perfect Fluids. Basic Ideas of Wing Theory: Flow Around an
   Airfoil. Vol. II of Aerodynamic Theory, div. E, ch. II,
   sec. 10, W. F. Durand, ed., Julius Springer (Berlin), 1935,
   pp. 48-53.

2. Brown, Clinton E.: Theoretical Lift and Drag of Thin Triangular
   Wings at Supersonic Speeds. NACA TN No. 1183, 1946.

3. Evvard, John C.: Theoretical Distribution of Lift on Thin Wings
   at Supersonic Speeds (An Extension). NACA TN No. 1585, 1948.
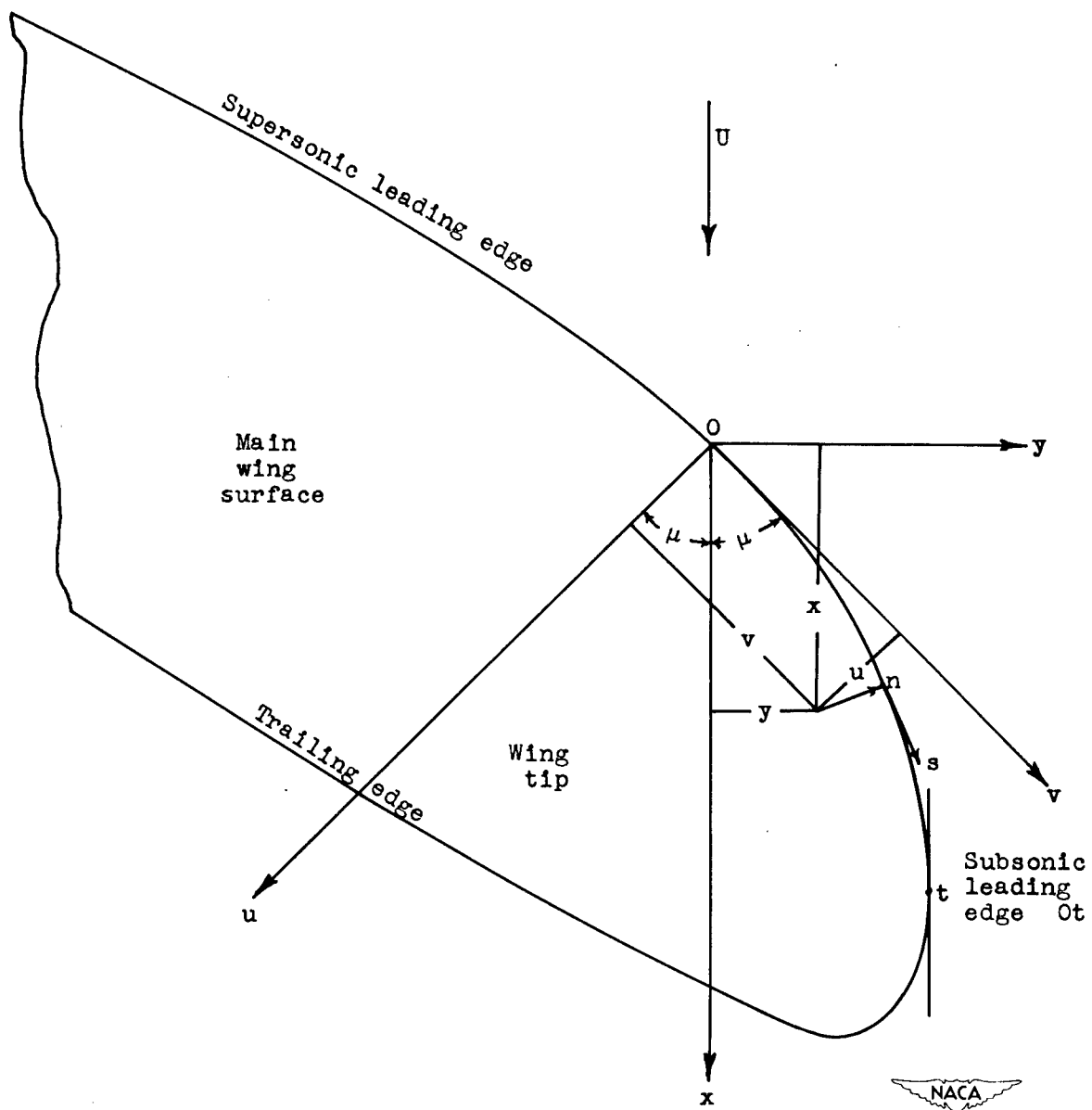
Figure 1. - Coordinate system used in analysis of wing tip.

$$R = \frac{\overline{QB}}{\overline{PQ}} = \frac{V}{u - u_2}$$

$$n = \frac{V}{R} \sin{(\theta + \mu)}$$
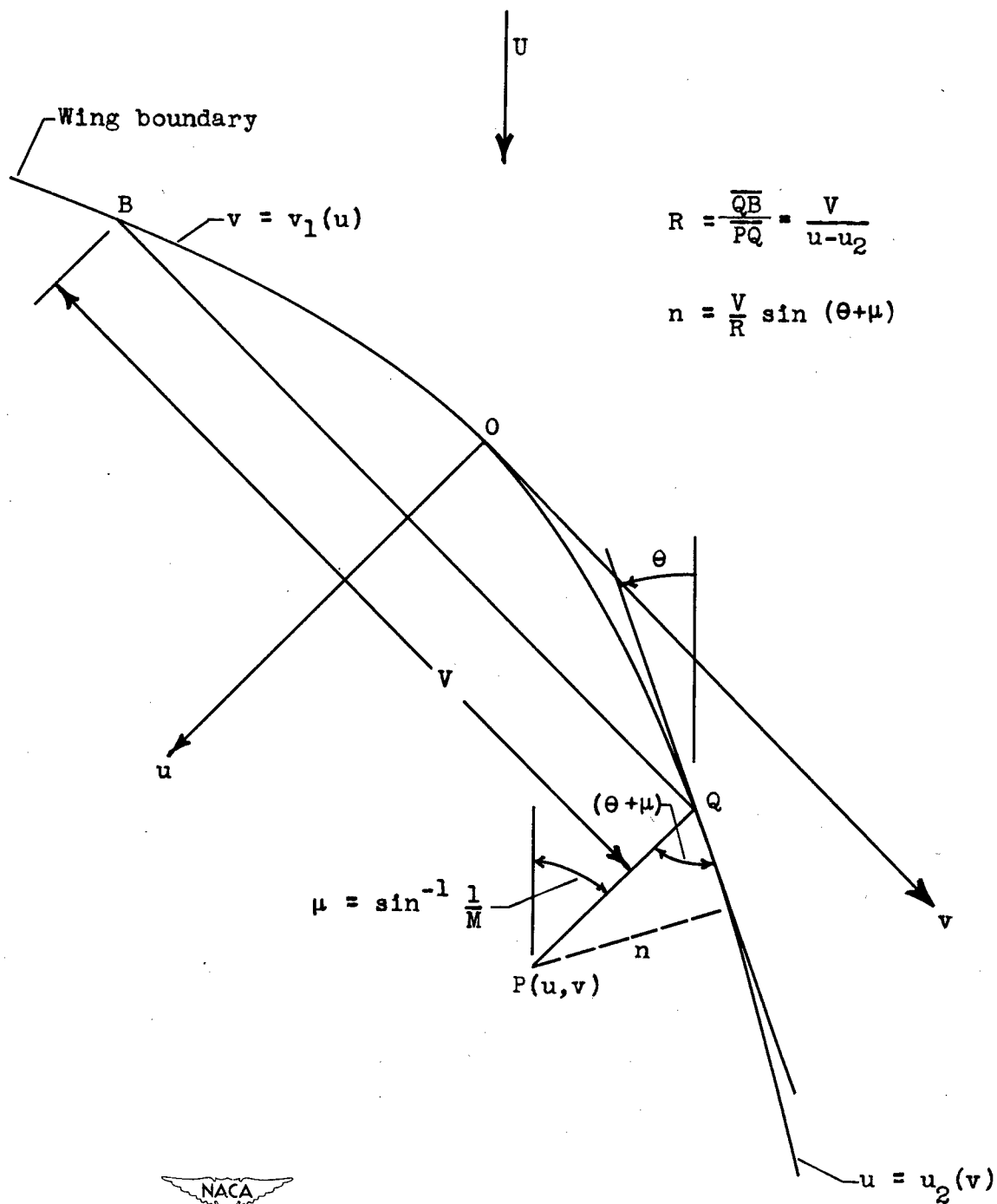
Figure 2. - Geometric relation between R and n.
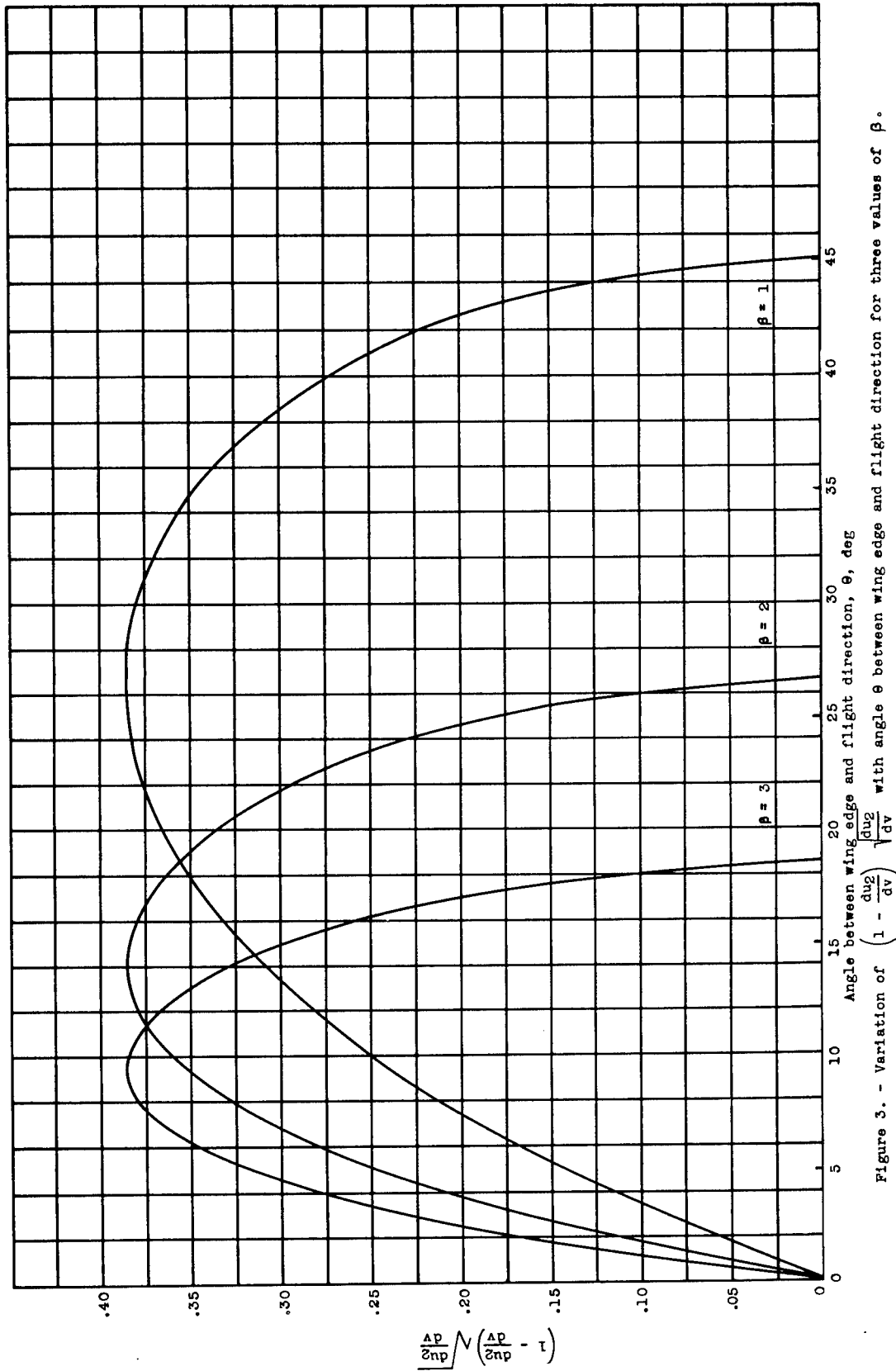
Figure 3. - Variation of $\left(1 - \dfrac{du_2}{dv}\right)\sqrt{\dfrac{du_2}{dv}}$ with angle θ between wing edge and flight direction for three values of β.

1001

u

Supersonic
leading edge

θ_1

$v_1 = k_1 u$

Trailing
edge
$v = k_1 u + b$

c

u

$u = u_2(v)$

(v_t, u_t)

v

NACA
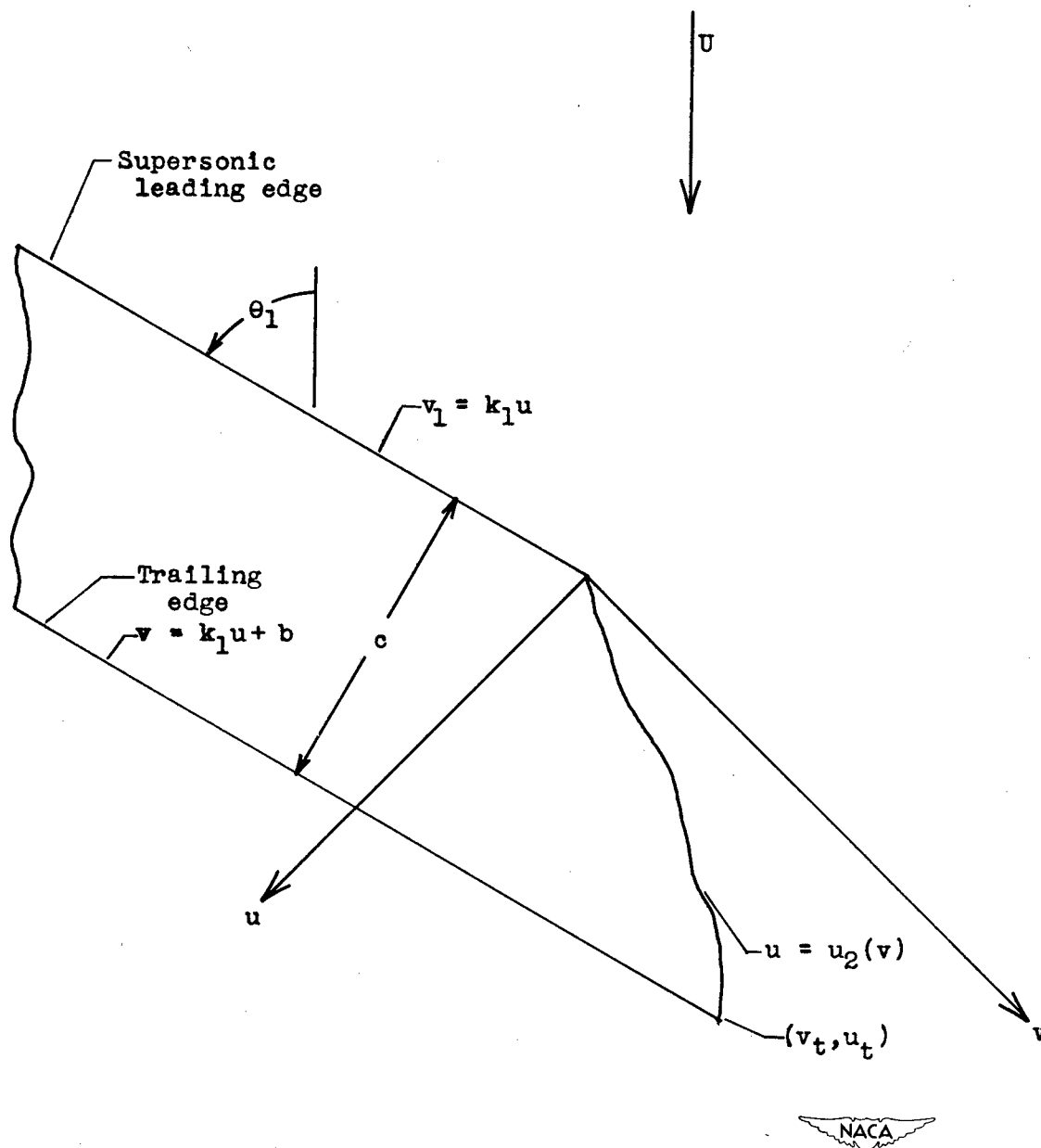
Figure 4. - Wing with straight supersonic leading edge and
generalized subsonic leading edge $u_2(v)$.
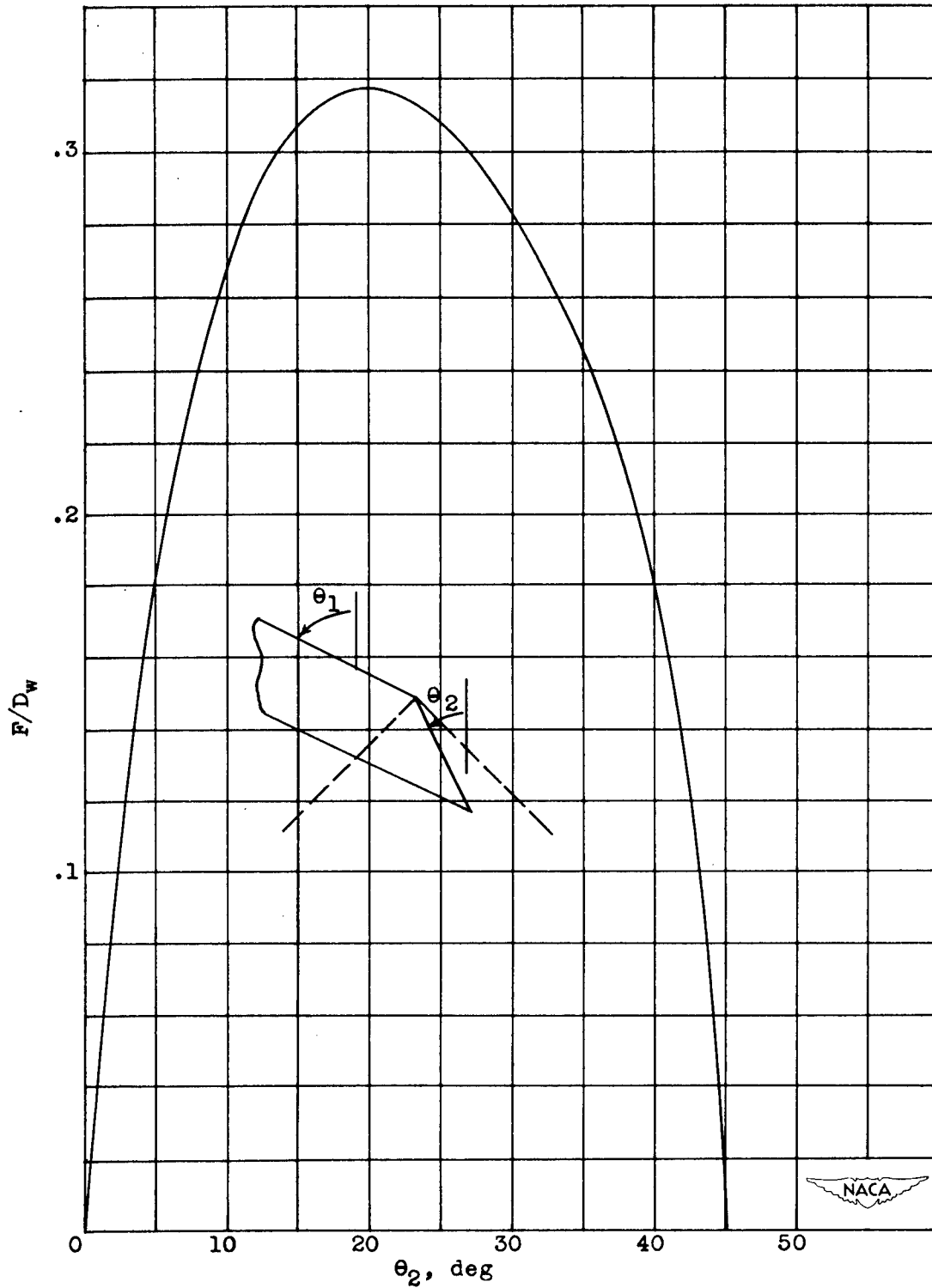
Figure 5. - Variation of F/D_W for tip of trapezoidal wing with $\theta_1 = 65^\circ$ at $M = \sqrt{2}$.
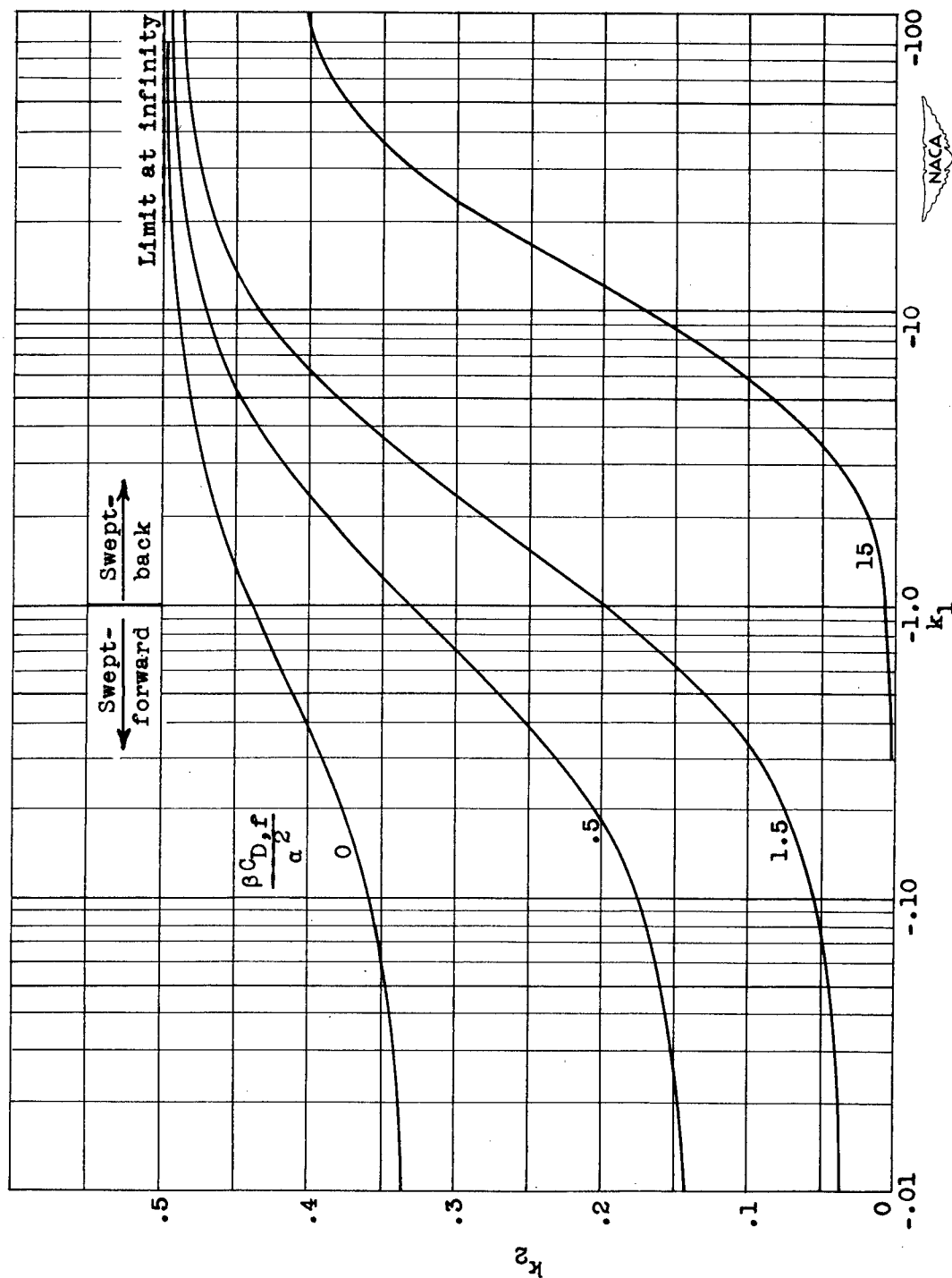
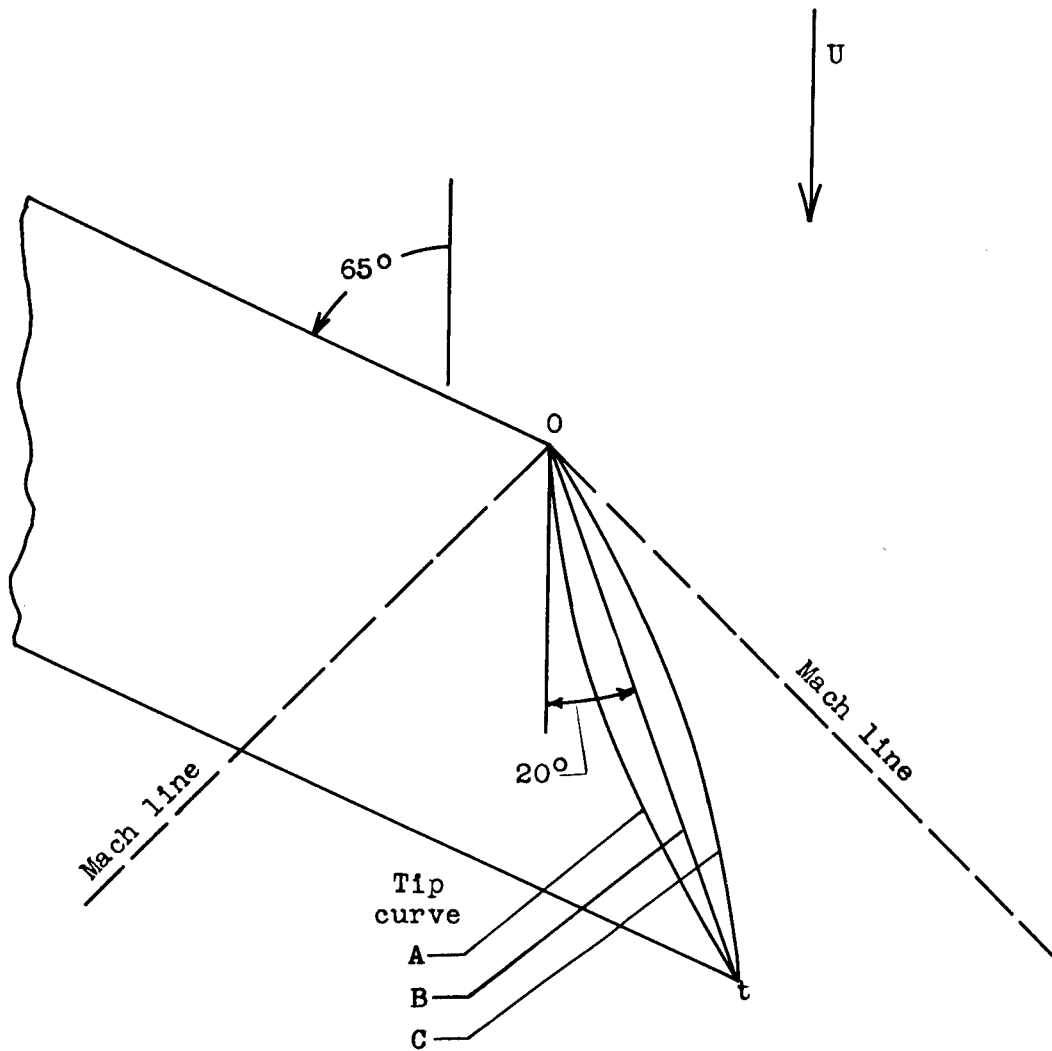Figure 6. - Variation of k_2 with k_1 for maximum lift-drag ratio of trapezoidal wing tips.

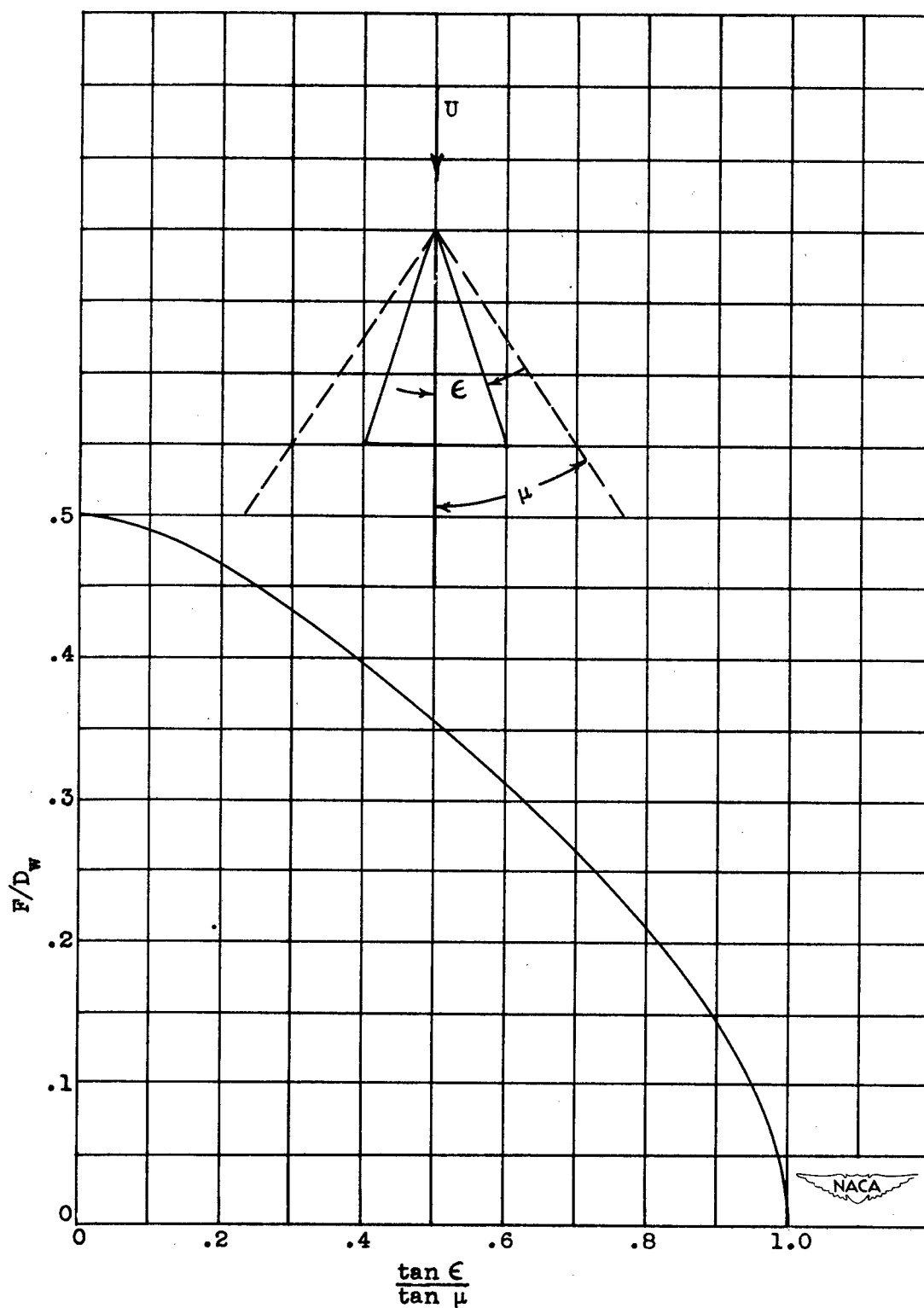Figure 7. – Wing tips analyzed for wing with $\theta_1 = 65°$ at $M = \sqrt{2}$.

1001

Figure 8. - Variation of F/D_W with apex angle for triangular
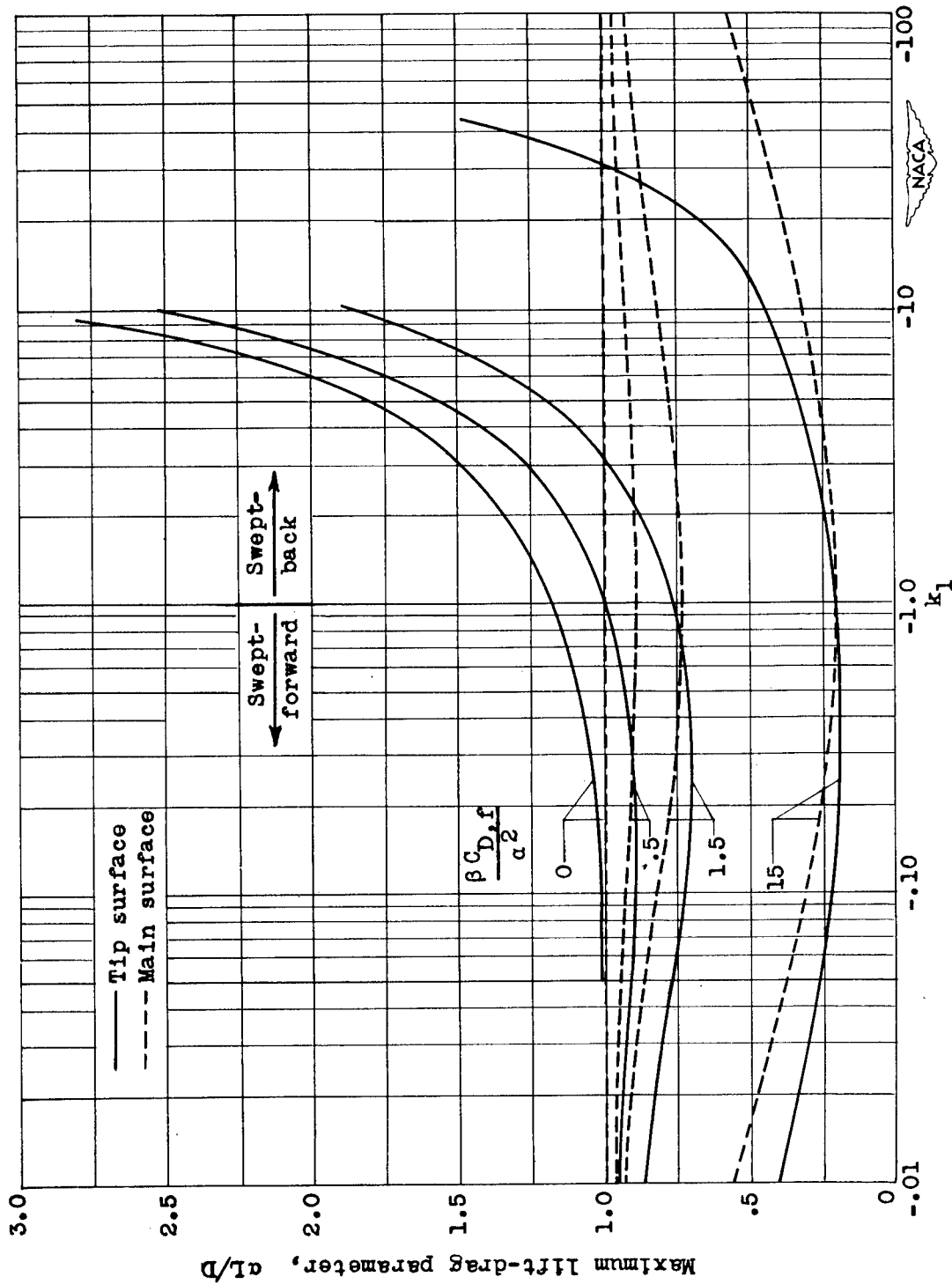wings. (Based on equations from reference 2.)

Figure 9. - Maximum lift-drag ratio for regions of trapezoidal wings when effects of leading-edge suction and friction drag are considered.
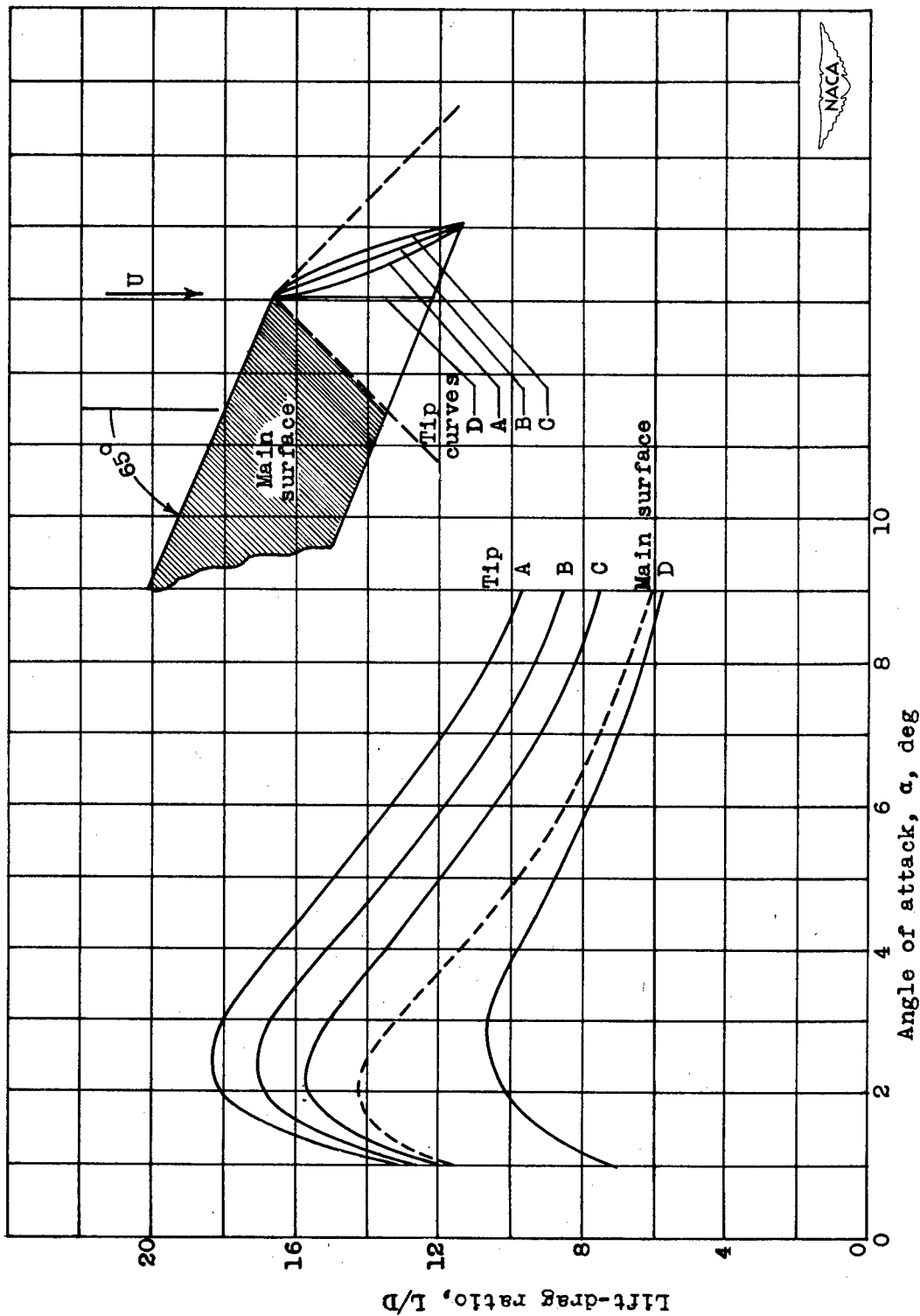
Figure 10. – Variation of lift-drag ratio with angle of attack at $M = \sqrt{2}$ and $C_{D,f} = 0.005$.